



Contents lists available at ScienceDirect

Bioorganic & Medicinal Chemistry

journal homepage: www.elsevier.com/locate/bmc

Synthesis and preliminary evaluation of ^{18}F -icotinib for EGFR-targeted PET imaging of lung cancer

Xinmiao Lu^{a,b}, Cheng Wang^{c,d}, Xiao Li^e, Peilin Gu^{a,b}, Lina Jia^{a,*}, Lan Zhang^{a,*}

^a Shanghai Institute of Applied Physics (SINAP), Chinese Academy of Sciences, Shanghai 201800, PR China

^b University of Chinese Academy of Sciences, Beijing 100049, PR China

^c Department of Nuclear Medicine, Ren Ji Hospital, School of Medicine, Shanghai Jiao Tong University, Shanghai 200127, PR China

^d Institute of Nuclear Medicine, School of Medicine, Shanghai Jiao Tong University, Shanghai 200127, PR China

^e Department of Nuclear Medicine, Changhai Hospital, Shanghai 200433, PR China

ARTICLE INFO

Keywords:

EGFR
NSCLC
PET imaging
 ^{18}F -icotinib
Click reaction

ABSTRACT

Epidermal growth factor receptor (EGFR) has emerged as an attracting target in the field of imaging and treatment for non-small cell lung cancer (NSCLC). Radiolabeled EGFR-tyrosine kinase inhibitors (EGFR-TKIs) specifically targeting EGFR are deemed as promising probes for the imaging of NSCLC. This study aimed to label icotinib (one kind of EGFR-TKI) with ^{18}F through click reaction to develop a new EGFR-targeting PET probe- ^{18}F -icotinib. ^{18}F -icotinib was obtained in 44.81% decay-corrected yield in 100 min synthesis time with 34 GBq/ μmol specific activity and > 99% radiochemical purity at the end of synthesis. The identity of the product was confirmed by co-injection with ^{18}F -icotinib and ^{19}F -icotinib. The Log P was 1.28 ± 0.04 ($n = 6$). The tracer displayed excellent stability after incubation for 4 h in vitro. ^{18}F -icotinib showed satisfying binding ability to A549 NSCLC cells, which could be inhibited by icotinib. PET imaging studies demonstrated a specific uptake of the radiotracer ($0.90 \pm 0.24\%$ ID/g) in A549 tumor-bearing mice, while lower uptake was observed in heart, lung and spleen at 1.5 h post injection. Immunohistochemical staining confirmed that the A549 tumor was EGFR-positive. Therefore, we considered that ^{18}F -icotinib was a highly promising compound for EGFR-based tumor PET imaging.

1. Introduction

Lung cancer has the highest morbidity and mortality all over the world. Non-small cell lung cancer (NSCLC) accounting for > 80% of lung cancer is one of the most fatal diseases with a low five-year survival rate.¹

Epidermal growth factor receptor (EGFR) was overexpressed on the surface of NSCLC cells^{2,3} and closely related to the neovascularization, proliferation, metastasis and invasion of tumor cells.^{4,5} Targeted therapy against EGFR using EGFR-tyrosine kinase inhibitor (EGFR-TKI)⁶ is effective in clinical treatments due to their great specificity and targeting ability to EGFR.^{7–9}

Positron emission tomography (PET) imaging technology especially combined with computed tomography (CT) is the most advanced imaging technology with great specificity and sensitivity. The specific sensitivity of radiolabeling EGFR-TKI to EGFR has been already exploited to design PET probes for diagnosis and imaging for NSCLC (Fig. 1), yet with some inadequate more or less. For example, ^{18}F -

gefitinib has high non-specific absorption and strong background signal in in vivo evaluation.¹⁰ ^{11}C -gefitinib has obvious accumulation in the intestine, and the application is limited by nuclide ^{11}C , which only has a half-life of 20 min.¹¹ ^{18}F -FEA-erlotinib reported in 2017 displayed extremely high uptake in liver and intestine, and the accumulation in the heart and kidneys was also obvious, according to the biodistribution studies.¹² ^{11}C -erlotinib is the most promising PET probe,^{13,14} it can detect the lymph node metastases which can't be distinguished by ^{18}F -FDG. But it still has high accumulation in the intestine and was also limited by the usage of ^{11}C .

Icotinib¹⁵ is one kind of EGFR-TKI molecule with quinoline structure, which has great specificity and targeting ability to EGFR. Pharmacokinetic analysis shows that the in vivo half-life of icotinib is 6 h (half-life of gefitinib \approx 40 h and half-life of erlotinib \approx 36 h¹⁶), and the concentration in blood reaches the peak in 2 h post injection (p.i.),¹⁷ which demonstrates that icotinib has higher potential to be the precursor to design a PET probe. Since the in vivo effective time of a probe only needs to meet the time required for specific accumulation and

* Corresponding authors at: P. O. Box 800-204, Shanghai 201800, PR China.

E-mail addresses: jialina@sinap.ac.cn (L. Jia), zhanglan@sinap.ac.cn (L. Zhang).

<https://doi.org/10.1016/j.bmc.2018.12.034>

Received 7 November 2018; Received in revised form 24 December 2018; Accepted 27 December 2018

0968-0896/ © 2018 Published by Elsevier Ltd.

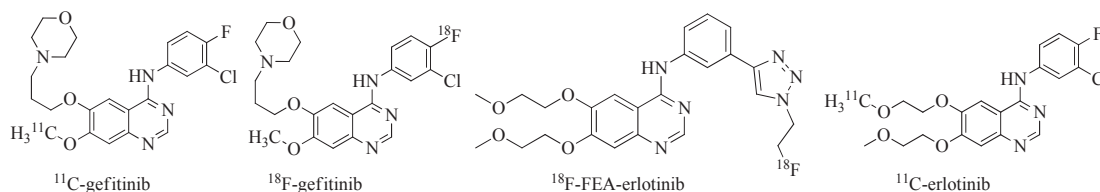


Fig. 1. EGFR-TKI PET imaging probes.

diagnostic observation. Longer in vivo retention time makes no sense but produces excess radiation damage. Meanwhile, icotinib has a crown ether structure, which could provide higher hydrophilicity. Therefore, icotinib labeled with ^{18}F may show great potential to improve the quality of NSCLC PET imaging. So it is valuable to use icotinib as the precursor to develop a PET probe targeting EGFR.

The copper(I) catalyzed cycloaddition between azides and alkynes (CuAAC) to form 1,2,3-triazoles is the most famous ‘click reaction’. Because of the advantage of mild reaction conditions, tolerance of solvents and pH, high chemoselectivity and perfect regioselectivity,^{18,19} this reaction was introduced into the field of radiopharmaceutical and has achieved great success, especially for ^{18}F labeled PET probes. Several innovated PET probes have been developed based on CuAAC reaction.^{20–22} Notably, ^{18}F -HX₄ prepared by CuAAC reaction is in clinical studies for non-invasive detection of hypoxia in patients with head and neck, or lung cancer.²² Therefore, the aim of this study is to synthesize the EGFR targeting PET probe based on icotinib via CuAAC reaction and evaluate its practicality as a PET tracer in NSCLC.

2. Experimental section

2.1. General information

All reagents were purchased commercially from Sinopharm Chemical Reagent Co, Ltd. (Shanghai, China) except for special instructions. Icotinib was purchased from Adooq Bioscience. All reagents and solvents were used without further purification unless noted otherwise. Agilent 1100 High Performance Liquid Chromatography (HPLC) equipped with UV-Vis absorbance detector and radioactive detector was used for purification and quality control of ^{18}F -icotinib with absorbance at 254 nm. A semi-preparative column (Agilent XDB C18, 9.4 × 300 mm, with a flow rate of 2 mL/min, UV at 254 nm) was used in the experiments. The mobile phase of HPLC was H₂O (A) and acetonitrile (B).

A549 xenograft mice were obtained from National Rodent Experimental Animal Seed Center (Shanghai, China). 5×10^6 A549 cells in 100 μL phosphate-buffered saline (PBS) were inoculated subcutaneously into the shoulder of 6–8 week-old male athymic nu/nu nude mice. Tumor was taken out and crushed into 1 mm pieces after achieving 5 mm, then were surgically implanted subcutaneously under isoflurane anaesthesia to the athymic nu/nu nude mice. Tumors were allowed to grow to 5–10 mm before imaging studies were commenced.

2.2. Synthesis of reference compound ^{19}F -icotinib (4)

2.2.1. Synthesis of 2-fluoroethyl-4-toluenesulfonate (1)

2-Fluoroethanol (20 mL) and p-toluenesulfonyl chloride (7.15 g, 37.53 mmol) was added to 80 mL dichloromethane and reacted under the catalysis of 17.40 mL triethylamine and 0.20 g 4-dimethylaminopyridine (DMAP) at room temperature for 24 h. 2-Fluoroethyl-4-toluenesulfonate (1) (4.23 g, 19.40 mmol) was collected in 51.70% yield after purifying by column chromatography.

2.2.2. Synthesis of 1-azido-2-fluoroethane (2)

2-Fluoroethyl-4-toluenesulfonate (1) (4.23 g, 19.40 mmol) and sodium azide (3.78 g, 58.15 mmol) was added into 55 mL DMF and

reacted at room temperature until 2-fluoroethyl-4-toluenesulfonate (1) disappeared. The reaction mixture was filtered, and the filtrate containing 1-azido-2-fluoroethane (2) was used without isolation for subsequent reactions.

2.2.3. Synthesis of ^{19}F -icotinib (4)

To a stirred solution of copper sulfate (0.15 mmol) and sodium ascorbate (0.30 mmol) in 12 mL PBS (pH 6.0) was added a solution of icotinib (3) (26.50 mg, 0.068 mmol) in DMF (1 mL). After addition of 2-fluoroethylazide (2) (0.70 mmol) in 2 mL DMF, stirring was continued at 50 °C for 1 h. The reaction mixture was quenched with H₂O (30 mL), and extracted with ethyl acetate (3 × 20 mL). After drying over sodium sulfate, the solvent was removed with reduced pressure to yield 31.21 mg click product ^{19}F -icotinib (4) in 95.71% ‘click reaction’ yield.

TOF-ESI-MS (ESI) [M + H]⁺ 481.15, [M + Na]⁺ 503.15, (C₂₄H₂₅O₄N₆F, calculated molecular weight [MW] = 480.49).

¹H NMR (400 MHz, CD₃OD): δ 8.65(s, 1H), δ 8.54(s, 1H), δ 8.34(s, 1H), δ 8.22(s, 1H), δ 7.93–7.97(t, 1H), δ 7.57–7.58(d, 1H), δ 7.46–7.50(t, 1H), δ 7.33(s, 1H), δ 4.75–4.98(t, 2H), δ 4.31–4.34(m, 4H), δ 3.77–3.82(m, 4H), δ 3.66(m, 4H), δ 2.90(s, 1H), δ 2.74(s, 1H). ¹³C NMR (100 MHz, CD₃OD): δ 162.79, δ 157.11, δ 156.47, δ 153.82, δ 150.25, δ 146.98, δ 140.50, δ 131.39, δ 130.69, δ 130.11, δ 129.54, δ 122.35, δ 122.07, δ 120.81, δ 119.08, δ 110.74, δ 83.20, δ 81.52, δ 73.42, δ 70.94, δ 70.85, δ 70.43, δ 69.26, δ 68.87

2.3. Synthesis of ^{18}F -icotinib (7)

2.3.1. Synthesis of 2-azidoethyl-4-toluenesulfonate (5)

1,2-Bis(tosyloxy)ethane (1.24 g, 3.35 mmol) was added to 100 mL DMF, then sodium azide (total 0.22 g, 3.38 mmol) was added every 0.5 h, (0.073 g × 3). The mixture reacted at room temperature for 24 h. 2-azidoethyl-4-toluenesulfonate (5) (0.46 g, 1.91 mmol) was obtained after purifying by column chromatography in 57.01% yield.

¹H NMR (400 MHz, CD₃OD): δ 7.83–7.85(t, 2H), δ 7.48–7.50(t, 2H), δ 4.15–4.18(t, 2H), δ 3.51–3.53(t, 2H), δ 2.48(s, 3H).

2.3.2. Synthesis of ^{18}F -1-azido-2-fluoroethane (6)

^{18}F -fluoride (n.c.a) (5–20 mCi) was captured on QMA Cartridge and was eluted with 2 mL mixture containing 28.8 mg K₂2.2 and 6.8 mg K₂CO₃ dissolved in 1.92 mL acetonitrile and 0.08 mL H₂O into reaction vial. The ^{18}F -fluoride/K₂CO₃/K₂2.2 mixture was dried three times by azeotropic distillation with dried acetonitrile under nitrogen purge at 115 °C in metal bath. After cooling down, 5.0 mg 2-azidoethyl-4-toluenesulfonate (5) in 0.4 mL of acetonitrile was added into dried ^{18}F -F⁻. The reaction vessel was sealed and heated to 115 °C for 10 min. After cooling down, the mixture of product was distilled at 85 °C for 15 min. Distilled product was collected to obtain ^{18}F -1-azido-2-fluoroethane (6) solution (3.0–12 mCi).

2.3.3. Synthesis of ^{18}F -icotinib (7)

^{18}F -1-azido-2-fluoroethane (6) (200 μL) and icotinib 3 (diluted in 300 μL DMF) were added to 200 μL PBS (pH = 6) and reacted under the catalysis of 0.5 M copper sulfate and 1.5 M sodium ascorbate for 15 min. The mixture was then filtered by a 0.22 μm filter membrane and the radiolabeling yield of click reaction was determined by radio-HPLC. The relative percentage content of the peak of ^{18}F -icotinib (7)

was determined by radio-HPLC with the normalization method of peak area. The filtered mixture was diluted with 6 mL water, and the ^{18}F -icotinib was trapped on a Sep-Pak light C18 cartridge, which was then rinsed with water (6 mL). The ^{18}F -icotinib was then eluted with 400 μL acetonitrile and diluted with 500 μL water. The product was isolated via semi-preparative radio-HPLC. The gradient was 0–15 min–16 min–23 min–24 min, 65%–65%–30%–30%–65% (A), 35%–35%–70%–70%–35% (B) and the flow rate was 2 mL/min. The ^{18}F -icotinib fraction was collected and diluted with water (8 mL). ^{18}F -icotinib was trapped on a Sep-Pak light C18 cartridge and rinsed with water (6 mL), then ^{18}F -icotinib was eluted by 300 μL ethanol. After removing part of ethanol, the product was formulated with 0.9% NaCl (containing 10% ethanol) for further use.

Since the use of copper was deemed as the default of click reaction, the concentration of copper ions in the preparation was tested using ICP-MS.

We also optimized the condition of click reaction, such as reaction temperature, precursor concentration and catalyst dosage, to get the highest radiolabeling yield.

2.4. Octanol/water partition coefficient

To determine the lipophilicity of ^{18}F -icotinib, 5 μL formulated ^{18}F -icotinib was added into the mixture of 595 μL PBS (pH 7.4) and 600 μL octanol. The mixture was vigorously vortexed for 2 min followed by centrifugation (12000 rpm, 5 min). From each layer, an aliquot of 100 μL was removed and counted in a γ -counter. The partition coefficient (log P) was then calculated as a ratio of counts in the octanol fraction to the counts in the water fraction. The experiment was repeated 6 times.

2.5. In vitro stability

The formulated ^{18}F -icotinib was incubated in 0.5 mL PBS (pH = 7.4) and 0.5 mL mouse serum for 4 h at 37 °C. The in vitro stability of the probe at different time points (including 0.5 h, 1 h, 2 h, 3 h and 4 h) was analyzed by radio-thin-layer chromatography (radio-TLC) (silica gel; methanol/ethyl acetate, 1:1 [v/v]; R_f = 0.5). Each test had a parallel sample. The in vitro stability of the probe in mouse serum and PBS after incubating for 4 h was also analyzed by radio-HPLC.

2.6. In vitro cell uptake

A549 Cells were grown in DMEM containing 10% fetal calf serum and antibiotics (penicillin) under 37 °C, 5% CO₂. A549 cells were seeded 24 h prior to the experiment in DMEM medium in 24-well plates at densities of 1×10^5 cells per well. On the day of the experiment, 15 μCi (50 μL) of ^{18}F -icotinib was added to the cells for the study group, while 15 μCi (50 μL) of ^{18}F -icotinib and 10 μg icotinib (50 μL) were added for the control group. After being incubated at 37 °C for 60 min, culture was removed and cells were washed twice with cold PBS to remove the free probes. Cells were dissolved with 1 mL NaOH (1.0 M)

and the wells were washed twice with PBS. The solution was transferred into a counting tube and the radioactivity was measured with a γ counter. The uptake fractions of ^{18}F -icotinib were calculated as percentage of applied dose per million cells. Sextuplet measurements were applied in this experiment.

2.7. PET-CT imaging

MicroPET-CT imaging was performed on A549 xenograft mice using a microPET/CT scanner (SuoerNova). All of the animal experiments followed the specifications for laboratory animal studies provided by Renji Hospital, Shanghai Jiao Tong University. Mice bearing A549 tumor were injected with approximately 1.3–1.5 MBq, 150 μL of ^{18}F -icotinib via the tail vein. To validate the specificity of ^{18}F -icotinib, mice with A549 tumor were injected with excess fold of icotinib (0.1 mg, 200 μL) via the tail vein before the administration of ^{18}F -icotinib. Then mice were anesthetized with 5% isoflurane delivered in 66%/33% nitrogen/oxygen prior to performing PET imaging experiments and the images at 1.5 h p.i. were reconstructed with the three dimensional ordered-subset expectation maximization (OSEM) algorithm.

Small-animal CT imaging was performed for anatomical reference and a 3 min acquisition was performed after PET. Mice were anesthetized with isoflurane (1–2%) throughout the period of imaging.

2.8. Immunohistochemical analysis

Mice bearing A549 tumor were sacrificed. The tumor tissues were extracted for analyzing the expression status of EGFR. Formalin-fixed, paraffin-embedded tumor tissue sections (thickness, 4–7 μm) were deparaffinized in xylene and rehydrated in gradient ethanol. Heat-induced antigen retrieval was conducted in 10 mmol/L citrate buffer. Endogenous peroxidase was blocked by incubation with 3% hydrogen peroxidase for 10 min. The slides were then incubated with primary antibodies rabbit anti-EGFR (1:100, Abcam, ab52894), followed by peroxidase conjugated secondary antibodies for 0.5 h at 37 °C. Color development was treated with DAB (3, 3'-diaminobenzidine tetrahydrochloride) and counterstaining was performed with hematoxylin. The optical density (OD) value was measured by image analysis.

3. Results

3.1. Chemistry and radiochemistry

The reference compound ^{19}F -icotinib (**4**) was synthesized in a three-step procedure as shown in Fig. 2. ^{19}F -icotinib (**4**) was obtained with > 99% purity (HPLC) without further purification. The structure was characterized by MS and NMR spectroscopy (see more in Supporting information).

2-Azidoethyl-4-toluenesulfonate (**5**), ^{18}F -1-azido-2-fluoroethane (**6**) and ^{18}F -icotinib (**7**) were synthesized as shown in Fig. 3. 2-Azidoethyl-4-toluenesulfonate (**5**) was obtained in a yield of 57.01%. ^{18}F -1-azido-2-fluoroethane (**6**) was prepared via nucleophilic fluorination of 2-

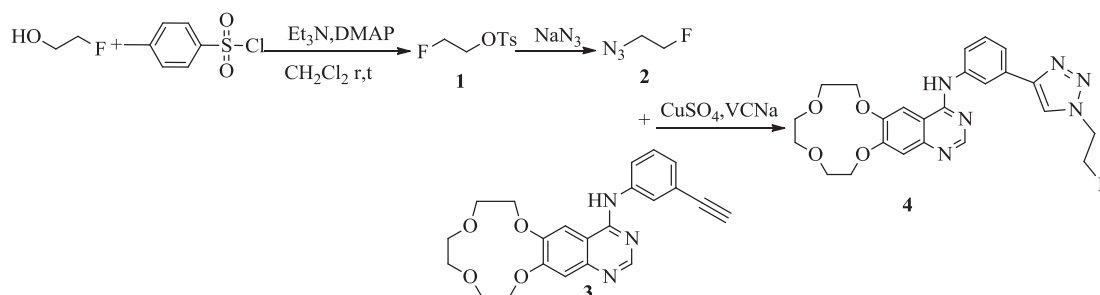


Fig. 2. The synthesis process of reference compound ^{19}F -icotinib (**4**).

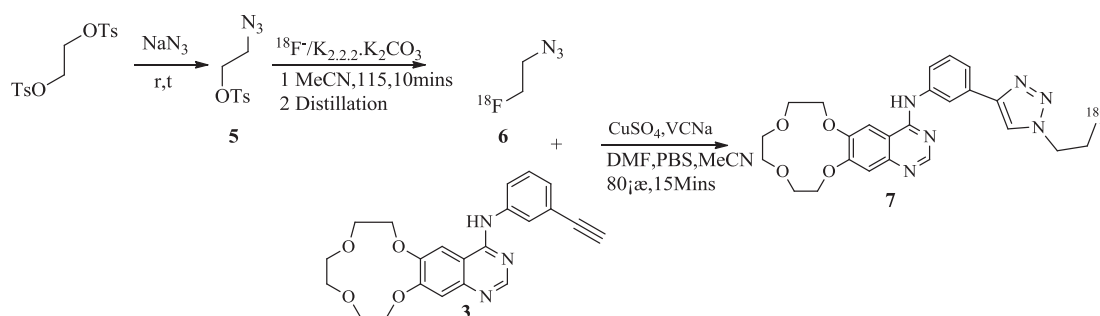


Fig. 3. Synthesis of 2-azidoethyl-4-toluenesulfonate (5), ¹⁸F-1-azido-2-fluoroethane (6) and ¹⁸F-icotinib (7).

Table 1

Yield of 'click' radiolabeling reaction of ¹⁸F-icotinib under different reaction conditions.

Entry	Icotinib/mg	CuSO ₄ /μL	Sodium ascorbate/μL	PBS/μL	Temperature/°C	Yield of 'click' radiolabeling*
1	1	20	20	67	50	18.4 ± 1.3% (n = 3)
2	1	60	60	200	50	33.3 ± 2.8% (n = 3)
3	2	20	20	67	50	19.9 ± 3.2% (n = 3)
4	2	60	60	200	50	43.6 ± 5.3% (n = 3)
5	4	60	60	200	50	71.1 ± 4.8% (n = 3)
6	4	60	60	200	80	> 99%

* Yields were determined by radio-HPLC.

azidoethyl 4-benzenesulfonate (5). The radiolabeling yield of (6) was > 99% and the distillation efficiency was > 72%. The radiochemical purity of ¹⁸F-1-azido-2-fluoroethane (6) after distillation was > 99% and chemical impurities such as K_{2.2.2} and labeling precursor could be removed from the labeling product and had no influence to the subsequent reaction.

The conditions of click reaction were optimized and the results were showed in Table 1. Under the optimized condition, ¹⁸F-icotinib was prepared in > 99% radiolabeling yield with the reaction condition of icotinib (0.01 mmol), CuSO₄ (3.0 equiv) and sodium ascorbate (9.0 equiv) reacting with ¹⁸F-1-azido-2-fluoroethane (6) in a solution of PBS (pH 6.0), DMF and acetonitrile (200 μL:300 μL:200 μL) for 15 min at 80 °C. After purification, ¹⁸F-icotinib was obtained in 44.81% decay-corrected yield in 100 min synthesis time with 34 GBq/μmol specific activity at the end of synthesis (EOS) and > 99% radiochemical purity. ¹⁸F-icotinib was identified by co-elution with reference compound ¹⁹F-icotinib (t_R = 12.65 min) by HPLC (Fig. 4).

The copper ion concentration of the formulated product determined by ICP-MS was 20 ppb, which fulfilled the requirements for intravenous

injection.

3.2. Octanol/water partition coefficient

The radioactivity counts distributing in the water layer and oil layer was recorded. The measured log P value of ¹⁸F-icotinib was 1.28 ± 0.04 (n = 6), according to our experiments.

3.3. In vitro stability

The in vitro stability of ¹⁸F-icotinib was determined by radio-TLC and radio-HPLC. The radio-TLC (see more in Supporting Information) and radio-HPLC results showed that ¹⁸F-icotinib kept completely intact after 4 h incubation in 0.01 M PBS (pH 7.4) and mouse serum. Stability analysis chromatograms of ¹⁸F-icotinib by HPLC after 4 h incubation were shown in Fig. 5.

3.4. In vitro cell uptake

The cellular uptake results showed the uptake of ¹⁸F-icotinib in the A549 cells harboring EGFR expression was high (19.50 ± 4.85% applied radioactivity per million cells (n = 6)). The uptake of ¹⁸F-icotinib in the A549 cells was reduced when cells were incubated with icotinib at the same time (10.59 ± 0.91% applied radioactivity per million cells (n = 6)). The result suggested that ¹⁸F-icotinib exhibited specificity for EGFR.

3.5. PET-CT imaging

The microPET-CT images of A549 xenograft mice at 1.5 h p.i. were shown in Fig. 6. Obvious accumulation of ¹⁸F-icotinib was seen in tumor, and the maximum SUV (Standardized Uptake Value) and average SUV in tumor were 0.65 and 0.35, respectively. The tumor uptake of ¹⁸F-icotinib at 1.5 h p.i. based on PET quantification was 0.90 ± 0.24 %ID/g. Tracer uptake was predominantly observed in the intestine (SUV_{max} = 25.87). The tracer was eliminated from the kidney rapidly (SUV_{max} = 0.91). There was no obvious uptake in the lung and muscle which corresponded to high tumor-to-lung and -muscle ratios (3.5, and 7.0 respectively). Negligible bone uptake (SUV_{max} = 0.05 at 1.5 h p.i.) was observed.

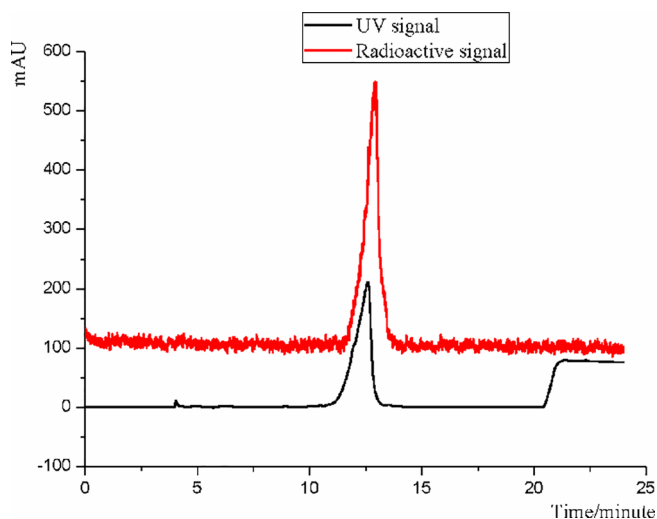


Fig. 4. HPLC analysis of ¹⁸F-icotinib (7) co-injected with ¹⁹F-icotinib (4).

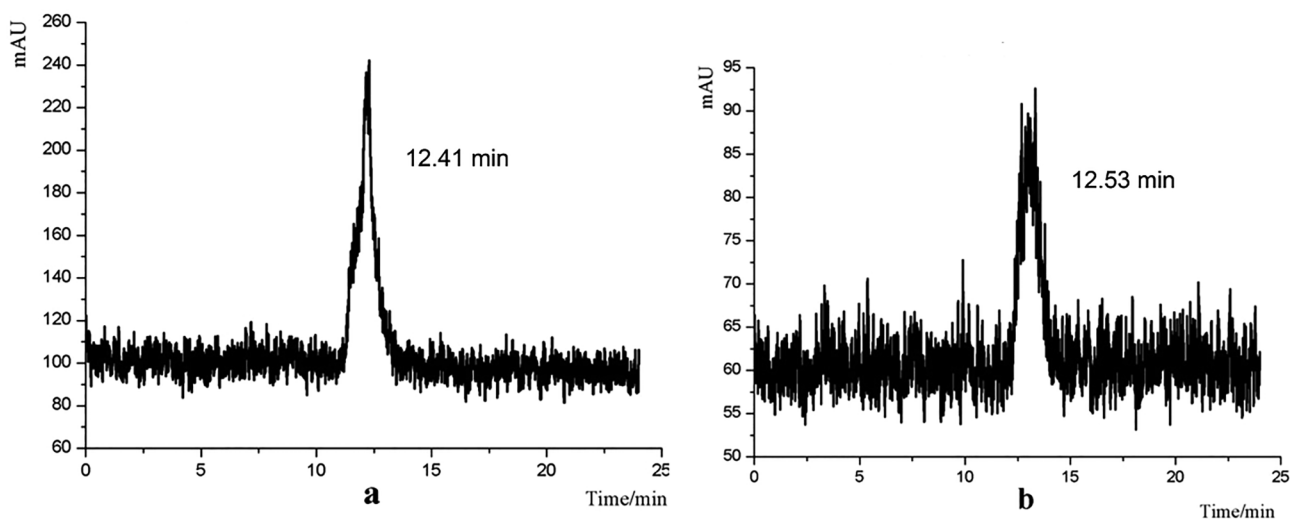


Fig. 5. The in vitro stability of ^{18}F -icotinib (7) in PBS (pH = 7.4) and mouse serum.

The excess icotinib will block the tumor EGFR, which would lead to the decreased accumulation of ^{18}F -icotinib in the tumor. So when icotinib was used as a blocker in PET imaging, radioactivity uptake in the tumor was dramatically reduced. The uptake in mice was $0.3 \pm 0.11\%$ ID/g, and the maximum SUV of tumor was 0.05 and the average SUV was 0.01 (35-fold decreased), respectively.

3.6. Immunohistochemical analysis

To validate the EGFR expression in A549 tumors harvested from the mice we used in PET imaging experiments, tumor specimens were analyzed for EGFR. Typical results of immunohistochemical analysis of A549 tumors were showed in Fig. 7, which indicated that in both blocked and unblocked imaging experiments, A549 tumors were EGFR-positive and there was no obvious difference of EGFR expression level. OD values of blocked and unblocked xenograft sections were 0.24 ± 0.02 (n = 6) and 0.27 ± 0.04 (n = 6), respectively.

4. Discussion

Targeted therapy with EGFR-TKI is effective for the clinical treatment of NSCLC. However, only patients with high expression and/or specific mutations of EGFR demonstrate high sensitivity to the EGFR-targeted therapy, an indiscriminate use of EGFR targeting drugs would make the overall efficiency poor. To achieve reasonable and effective therapy for NSCLC patients, reliable diagnosis and accurate images are of great values. In this study, we synthesized and biologically evaluated the EGFR targeting PET probe- ^{18}F -icotinib based on icotinib, which is a reversible EGFR-TKI and has been approved to be used in the treatment of advanced NSCLC in 2011 in China.

According to the structure activity relationship between icotinib and EGFR protein,^{23,24} the amino substituent and nitrogen atoms on the quinoline ring play a pivotal role in the drug efficacy. It is beneficial for the inhibitory activity of quinazoline EGFR-TKI that the radiolabeling of icotinib with the 'click reaction' between azides and alkynes to introduce of 1,2,3-triazoles to the 3'-position of icotinib molecules. So, ^{18}F -icotinib was synthesized using the efficient click reaction.

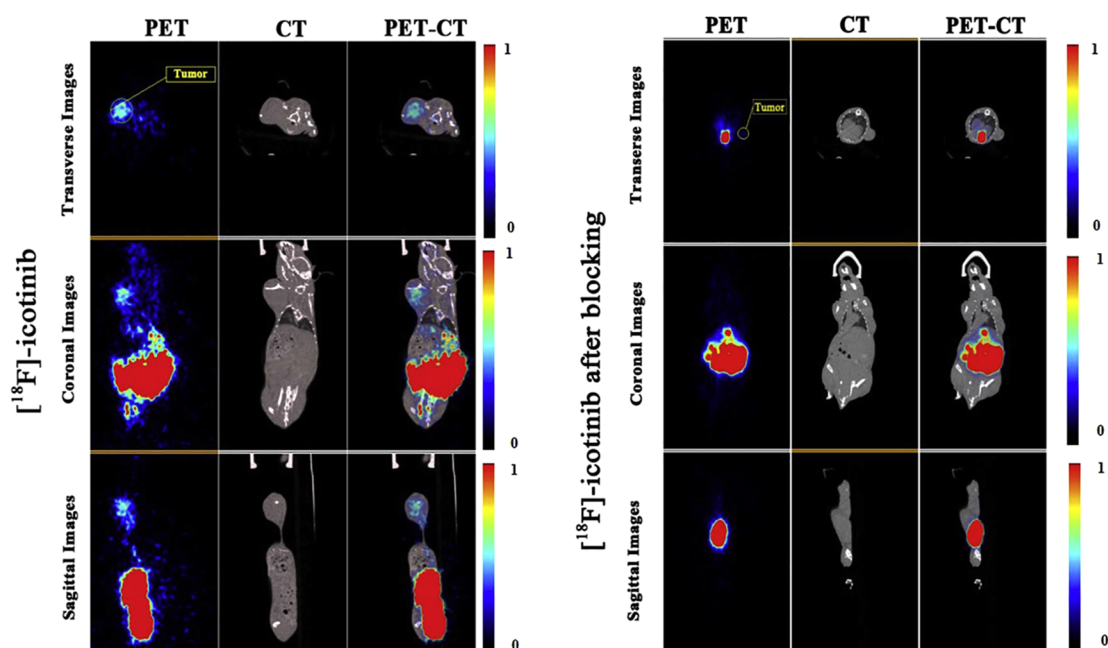


Fig. 6. MicroPET/CT images acquired at 1.5 h post-injection with 1.3–1.8 MBq ^{18}F -icotinib (7) in A549 xenograft mice anesthetized with 5% isoflurane.

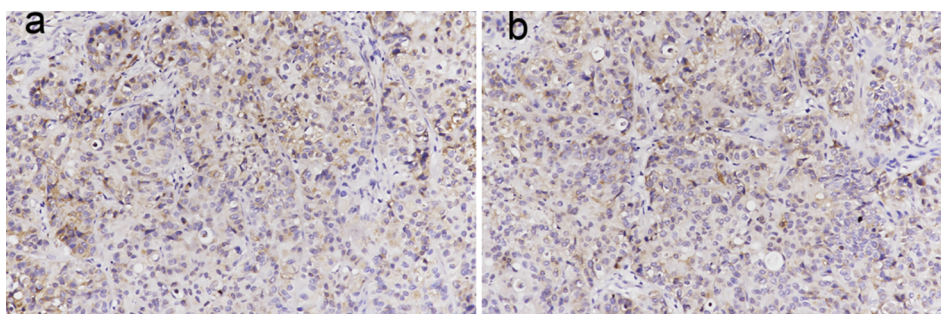


Fig. 7. Immunohistochemical staining of A549 tumors with anti-EGFR antibody. (a) Tumors in mice injected with ^{18}F -icotinib (7); (b) tumors in mice co-injected with ^{18}F -icotinib (7) and icotinib, (original magnification, $\times 200$).

According to the results given by the condition experiments in Table 1, it was evident that higher radiolabeling yield can be obtained by increasing reaction temperature, dosage of catalyst and concentration of icotinib. In short, thanks to the great virtue of click reaction, the results in both chemistry and radiochemistry process were extremely satisfying and the radiochemical yield (44.81%) and specific activity (34 GBq/ μmol) were also acceptable. From all aspects, it did help a lot to improve the nuclide utilization and lower the initial radioactivity of $^{18}\text{F}^-$.

The Log P value of ^{18}F -icotinib was 1.28 ± 0.04 ($n = 6$), which meant that the probe is a little lipophilic. And by all means, EGFR-TKIs drugs or probes generally reach their targets by passive diffusion through the cell membrane. Therefore the lipophilicity is generally necessary. Compared with ^{18}F -FEA-erlotinib reported recently, which was also labeled with ^{18}F via CuAAC reaction,¹² ^{18}F -icotinib demonstrated reduced radioactivity accumulation in the liver at their own observation time point ($0.96 \pm 0.21\% \text{ID/g}$ at 90 min p.i. to $15.2 \pm 3.7\% \text{ID/g}$ at 60 min p.i.), likely due to the lower lipophilicity of ^{18}F -icotinib (Log P value of ^{18}F -FEA-erlotinib was 2.36 ± 0.01). ^{18}F -icotinib kept totally intact after 4 h incubation. No defluorination or radioactive metabolic degradation was observed, which reflected the great in vitro stability of our probe. The cell assays demonstrated that ^{18}F -icotinib exhibited selectivity to EGFR which indicated that ^{18}F -icotinib was valuable for a further exploitation.

Here we showed that EGFR positive tumor could be detected by ^{18}F -icotinib PET imaging. Low accumulation in bone of ^{18}F -icotinib was observed in the PET images, which reflected the in vivo stability of our probe. High uptake was observed in the intestine, which was consistent with the metabolic process of the reported probes.^{10,11,25,26} So, further exploitation should be dedicated to optimizing the probe structure to reduce the accumulation in the intestine. The PET image indicated that probe existed rapid clearance from most of non-target organs such as lung, muscle, stomach, kidney and liver at 90 min p.i., which contributed to a low-uptake background and high tumor-to-normal organ contrast in the images. Co-injection of icotinib with ^{18}F -icotinib significantly reduced the uptake of ^{18}F -icotinib in tumors, which indicated the specific EGFR-mediated binding of this probe.

The results of immunohistochemical analysis demonstrated that the A549 tumors were EGFR-positive. The expression level of EGFR in tumors of both blocked and unblocked mice was comparable, which wouldn't bring about the significant difference of the uptake of ^{18}F -icotinib in PET imaging experiments. Thus, the specificity of EGFR-targeted imaging of our probe was further proved.

5. Conclusions

In conclusion, a new EGFR-specific probe ^{18}F -icotinib has been successfully prepared by click chemistry with great stability in PBS and mouse serum. PET imaging of A549 xenograft mice demonstrated that ^{18}F -icotinib had obvious tumor uptake and exhibited high tumor-to-normal tissue contrast. Hence, with further exploitation, ^{18}F -icotinib

has great potential to be translated into application in clinic as a reliable tool for tumor imaging.

Acknowledgement and declarations

None.

Funding

This study was financially supported by grants from the National Nature Science Foundation of China (NSFC) under Contract NO. 11505269 and the Strategic Priority and Research Program of Chinese Academy of Science under Contract NO. XDA02000000. The authors also acknowledge Shanghai Atom KeXing pharmaceutical Co., Ltd. for providing $^{18}\text{F}^-$.

Appendix A. Supplementary data

Supplementary data to this article can be found online at <https://doi.org/10.1016/j.bmc.2018.12.034>.

References

- Jemal A, Siegel R, Xu J, et al. Cancer statistics, 2010. *CA Cancer J Clin.* 2010;60(5):277–300.
- Dutu T, Michiels S, Fouret P, et al. Differential expression of biomarkers in lung adenocarcinoma: a comparative study between smokers and never-smokers. *Ann Oncol.* 2005;16(12):1906–1914.
- Sequist LV, Lynch TJ. EGFR tyrosine kinase inhibitors in lung cancer: an evolving story. *Annu Rev Med.* 2008;59(1):429–442.
- Chung CH, Ely K, McGavran L, et al. Increased epidermal growth factor receptor gene copy number is associated with poor prognosis in head and neck squamous cell carcinomas. *J Clin Oncol.* 2006;24(25):4170–4176.
- Gazdar AF. Activating and resistance mutations of EGFR in non-small-cell lung cancer: role in clinical response to EGFR tyrosine kinase inhibitors. *Oncogene.* 2009;28(1):24–31.
- Yewale C, Baradia D, Vhora I, et al. Epidermal growth factor receptor targeting in cancer: a review of trends and strategies. *Biomaterials.* 2013;34(34):8690–8707.
- Yung TK, Chan KC, Mok TS, et al. Activating mutations in the epidermal growth factor receptor underlying responsiveness of non-small-cell lung cancer to gefitinib. *New Engl J Med.* 2004;350(350):2129–2139.
- Zhu CQ, Santos GDC, Ding K, et al. Role of KRAS and EGFR as biomarkers of response to erlotinib in National Cancer Institute of Canada clinical trials group study BR.21. *J Clin Oncol.* 2008;26(26):4268–4275.
- Shepherd FA, Tsao MS. Unraveling the mystery of prognostic and predictive factors in epidermal growth factor receptor therapy. *J Clin Oncol.* 2006;24(7):1220–1221.
- Su H, Seimbill YG, Bodenstein C, et al. Evaluation of [^{18}F]-gefitinib as a molecular imaging probe for the assessment of the epidermal growth factor receptor status in malignant tumors. *Eur J Nucl Med Mol I.* 2008;35(6):1089–1099.
- Zhang MR, Kumata K, Hatori A, et al. [^{11}C]Gefitinib ([^{11}C]Iressa): radiosynthesis, in vitro uptake, and in vivo imaging of intact murine fibrosarcoma. *Mol Imaging Biol.* 2010;12(2):181–191.
- Huang S, Han Y, Chen M, et al. Radiosynthesis and biological evaluation of ^{18}F -labeled 4-anilinoquinazoline derivative (^{18}F -FEA-Erlotinib) as a potential EGFR PET agent. *Bioorg Med Chem Lett.* 2017;28(6):1143–1148.
- Memon AA, Weber B, Winterdahl M, et al. PET imaging of patients with non-small cell lung cancer employing an EGF receptor targeting drug as tracer. *Brit J Cancer.* 2011;105(12):1850–1855.
- Petrulli JR, Sullivan JM, Zheng MQ, et al. Quantitative analysis of [^{11}C]Erlotinib

- PET demonstrates specific binding for activating mutations of the EGFR kinase domain. *Neoplasia*. 2013;15(12):1347–1353.
15. Tan F, Shen X, Wang D, et al. Icotinib (BPI-2009H), a novel EGFR tyrosine kinase inhibitor, displays potent efficacy in preclinical studies. *Lung Cancer*. 2012;76(2):177–182.
 16. Ranson M, Hammond LA, Ferry D, et al. ZD1839, a selective oral epidermal growth factor receptor-tyrosine kinase inhibitor, is well tolerated and active in patients with solid, malignant tumors: results of a phase I trial. *J Clin Oncol*. 2002;20(9):2240.
 17. Zhao Q, Shentu J, Xu N, et al. Phase I study of icotinib hydrochloride (BPI-2009H), an oral EGFR tyrosine kinase inhibitor, in patients with advanced NSCLC and other solid tumors. *Lung Cancer*. 2011;73(2):195–202.
 18. Glaser M, Arstad E. “Click labeling” with 2-¹⁸F-fluoroethylazide for positron emission tomography. *Bioconjug Chem*. 2007;18(3):989–993.
 19. Li YL, Didier A. The copper(I)-catalyzed alkyne-azide cycloaddition (CuAAC) “click” reaction and its applications. An overview. *Coord Chem Rev*. 2011;255(23):2933–2945.
 20. Jia LN, Jiang DW, Cheng DF, Zhang L. Synthesis and preliminary evaluation of ¹⁸F-labeled bile acid compound for TGR5. *J Nucl Radiochem (in Chinese)*. 2014;36(4):247–252.
 21. Jia LN, Jiang D, Hu P, et al. Synthesis and evaluation of [¹⁸F]-labeled bile acid compound: a potential PET imaging agent for FXR-related diseases. *Nucl Med Biol*. 2014;41(6):495–500.
 22. Loon JV, Janssen MHM, Öllers M, et al. PET imaging of hypoxia with the new tracer ¹⁸F-HX₄: A phases 1 trial. *J Thorac Oncol*. 2009;4(9):S731–S732.
 23. Noolvi MN, Patel HM. A comparative QSAR analysis and molecular docking studies of quinazoline derivatives as tyrosine kinase (EGFR) inhibitors: a rational approach to anticancer drug design. *J Saudi Chem Soc*. 2013;17(4):361–379.
 24. Nandi S, Bagchi MC. Design of potent EGFR kinase inhibitors using combinatorial libraries. *Mol Simulat*. 2011;37(3):196–209.
 25. Hongyu Ren, Hongyu Ning, Jin Chang, et al. Evaluation of ¹⁸F-labeled icotinib derivatives as potential PET agents for tumor imaging. *J Radioanal Nucl Ch*. 2016;309(2):517–523.
 26. Galith A, Batel I, Olga S, et al. Identifying erlotinib-sensitive non-small cell lung carcinoma tumors in mice using [¹¹C]erlotinib PET. *EJNMMI Res*. 2015;5(1):4.